# GLACIER MONITORING: CORRELATION VERSUS TEXTURE TRACKING

*Charles-Alban Deledalle, Jean-Marie Nicolas, Florence Tupin* *Loïc Denis* *Renaud Fallourd, Emmanuel Trouvé*

Institut Telecom, Telecom ParisTech
CNRS LTCI
Paris, France

Observatoire de Lyon, CNRS CRAL
UCBL, ENS de Lyon, Université de Lyon
Lyon, France

Université de Savoie
LISTIC
Annecy, France

## ABSTRACT

Synthetic aperture radar (SAR) images provide scattering information which can be used under any weather conditions for glacier monitoring. Our purpose is to estimate a displacement field characterizing at each position the local speeds and orientations of the glacier displacement. Recent proposed methods build a vector field by tracking patches between two SAR images co-registered on static areas and sensed at different times [1, 2]. The tracking is performed either by evaluating the correlations or the similarities from one acquisition to the other. We propose to estimate locally the displacement vectors by using either the maximum correlation or a maximum likelihood estimator. This local estimation is then refined to provide a sub-pixelic result. The efficiency of both methods are compared.

***Index Terms***— Glacier monitoring, texture tracking, normalized cross-correlation, maximum likelihood

## 1. INTRODUCTION

The idea is to estimate at each position $s$ of the glacier a displacement vector $\overrightarrow{v_s}$, reflecting the speed and the orientation of the local movement. Let $A$ and $A'$ be two amplitude images co-registered on static areas and sensed at different times. We denote by $A_s$ and $A'_t$ the amplitudes measured respectively at position $s$ in reference image $A$ and at position $t$ in $A'$. The amplitude $A_s$ and $A'_t$ are assumed to follow a multiplicative speckle noise model such that:

$$A_s = \sqrt{R_s} \times \eta_s \quad (1)$$

$$A'_t = \sqrt{R'_t} \times \eta'_t \quad (2)$$

where $R_s$ and $R'_t$ are the underlying reflectivities at site $s$ and $t$, and $\eta_s$ and $\eta_t$ are two realizations of two random variables following a normalized Rayleigh distribution. The speckle is assumed to be spatially decorrelated inside each image and temporally decorrelated between both images. This last assumption holds according to the unstable scattering nature of the glacier surface. The realizations $\eta_s$ and $\eta_t$ are then decorrelated and analyzing the displacement vector $\overrightarrow{v_s}$ from the amplitude images $A$ and $A'$ is thus equivalent to analyzing it directly from the reflectivity images $R$ and $R'$.

Thanks to the French Research Agency (ANR) for supporting this work through the EFIDIR project (ANR-2007-MCDC0-04,www.efidir.fr) and the German Aerospace Agency (DLR) for the TerraSAR-X images (project MTH0232).

## 2. LOCAL ESTIMATION OF THE DISPLACEMENT

In order to estimate the displacement vector $\overrightarrow{v_s}$, the neighborhood of $s$ in the amplitude image $A$ and the neighborhood of $t = s + \overrightarrow{v_s}$ in $A'$ are assumed to be similar when the position $s$ corresponds to the position $t$. Indeed, corresponding objects are assumed to be seen in both images with similar patterns. That is the idea of texture tracking algorithms as proposed in [2]. In this paper, we define a new texture tracking algorithm that is able to deal with multiplicative speckle noise and we compare it to correlation based tracking. While correlation based tracking searches for correlated patches, texture tracking searches for patches with identical underlying reflectivities.

### 2.1. Correlation based tracking on SAR images (NCC)

In image processing, the correlation-like algorithms are often used for different tasks, such as image co-registration [3], displacement estimation on optical images [4, 5], or on amplitude SAR images [1, 6]. For SAR images, the centered Normalized Cross-Correlation (NCC) is generally used since it is robust to global changes between the reflectivites of the two SAR images. The NCC criterion is defined as:

$$\hat{\overrightarrow{v_s}} = \arg\max_{\overrightarrow{v_s} | t \in W_s} \frac{\sum_b \widetilde{A}_{s+b}\, \widetilde{A}'_{t+b}}{\sqrt{\sum_b \widetilde{A}^2_{s+b} \sum_b \widetilde{A}'^2_{t+b}}} \quad (3)$$

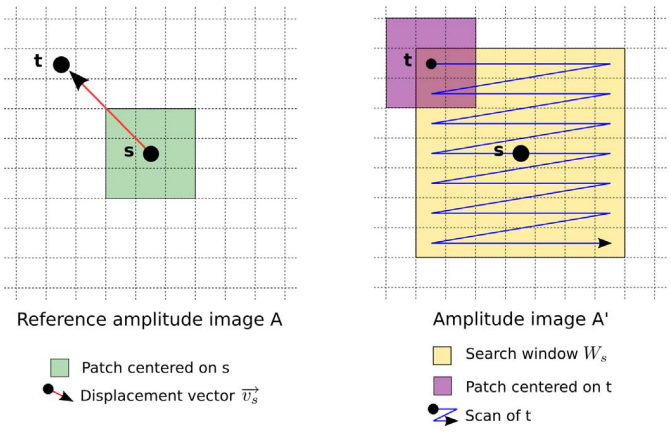


**Fig. 1**. Illustration of the proposed tracking method

$$\text{with} \quad \widetilde{A}_{s+b} = A_{s+b} - \overline{A}_s, \\ \widetilde{A}'_{t+b} = A'_{t+b} - \overline{A}'_t$$

where $\overline{A}_s$ and $\overline{A}'_t$ denote the mean over windows centered on pixel $s$ and $t$ respectively and $W_s$ is a rectangular window centered around $s$. The indexes $_{s+b}$ and $_{t+b}$ denote the $b$-th pixels in these respective patches.
While the NCC criterion is robust on optical images corrupted by additive noise, it is not suitable for SAR images corrupted by multiplicative noise, i.e. *speckle*. In next section, we propose to use instead texture tracking which is based on statiscally grounded.

### 2.2. Texture tracking on SAR images (ML)

As mentioned above, under the assumption of uncorrelated speckle noise, to analyze the displacement vector $\overrightarrow{v_s}$ from the amplitude images $A$ and $A'$ is equivalent to analyzing it directly from the reflectivity images $R$ and $R'$. Corresponding patches can then be obtained by evaluating the similarity of each values belonging to the patches, i.e $R_{s+b} = R_{t+b}$. In practice, the information $R_{s+b} = R_{t+b}$ is latent since the underlying reflectivity images $R$ and $R'$ are unknown. We estimate the patch similarities by using the likelihoods of $R_{s+b} = R_{t+b}$ for all $b$ with respect to the observations $A_{s+b}$ and $A'_{t+b}$. This leads to the following definition based on similarity likelihoods:

$$p(A, A'|\overrightarrow{v_s}) \triangleq \exp\left[-\sum_k \log\left(\frac{A_{s+b}}{A'_{t+b}} + \frac{A'_{t+b}}{A_{s+b}}\right)\right]. \quad (4)$$

This criterion has been introduced in [7] where its efficiency has been demonstrated for SAR image denoising. As shown in (4), this criterion has the ability to deal well with the multiplicative nature of the speckle noise since it is based on the speckle noise distribution. Similar criteria based on different assumptions have also been proposed in [2]. These similarities are then used to provide a local estimate of the displacement vector $\overrightarrow{v_s}$ in the maximum likelihood (ML) estimator [2]:

$$\hat{\overrightarrow{v_s}} = \arg \max_{\overrightarrow{v_s}|t\in W_s} p(A, A'|\overrightarrow{v_s}). \quad (5)$$

Figure 1 illustrates the procedure used in both methods. For each candidate vector $\overrightarrow{v_s}$ inside the window $W_s$, the correlation or similarity between the patch centered on $s$ and the patch centered on $t$ is evaluated. The local estimate of the displacement vector $\hat{\overrightarrow{v_s}}$ is then obtained by selecting the vector which maximizes the correlations or the likelihood to have the same reflectivities.

### 2.3. Measure of confidence

With classical correlation based tracking exposed in eq. (3), a measure of confidence for each estimated vector can be directly derived by the similarity peak, i.e. the higher value of the correlation in the search window $W_s$. In the specific case of glacier monitoring with SAR data, it has been shown that a displacement vector becomes reliable when its correlation peak becomes higher than $0.2$ [8]. Nevertheless, this approach cannot be applied with texture based tracking. Indeed with such tracking techniques the similarity peak is not bounded while the zero-mean normalized cross-correlation is bounded between $-1$ and $1$. The chosen approach, efficient with the two tracking techniques, consists in measuring the height of the similarity peak in comparison to its neighborhood. Erten *et al.* proposed to measure this height by the use of the following relation:

$$h_{peak} = \frac{\max(sim) - \text{mean}(sim)}{\text{mean}(sim) - \min(sim)} \quad (6)$$

where the *maximum*, the *minimum* and the *mean* are computed over the search window $W_s$. The higher the $h_{peak}$, the more confident the measure.

## 3. SUB-PIXELIC REFINEMENT

The displacement measure $\hat{\overrightarrow{v_s}}$ obtained with the approach shown on Figure 1 is discrete. To improve the precision, a sub-pixel measure $\hat{\overrightarrow{v_s}}' = \hat{\overrightarrow{v_s}} + \hat{\overrightarrow{v}}_{s,sub}$ is computed in two steps. First, the similarity function is approximated by a second order polynomial function over an interpolation block centered on the discrete similarity of the peak position. Secondly, the sub-pixel position $\hat{\overrightarrow{v}}_{s,sub}$ of the function maximum is obtained by cancelling the first derivatives of the interpolated function in lines and columns directions. Finally, the sub-pixel

| | Mean | | Std | |
|---|---|---|---|---|
| | NCC | ML | NCC | ML |
| Conf. $h_{peak}$ | 1.934 | 1.748 | 0.622 | 0.511 |
| Disp. zone 1 | 23.1 | 19.8 | 1.5 | 1.1 |
| Disp. zone 2 | 21.9 | 20.9 | 1.9 | 1.6 |

**Table 1**. Confidence and displacement measure statistics for 2008-09-29/2008-10-10 images pair. The displacement statistics are expressed in [cm/day].

displacement $\hat{\overrightarrow{v_s}}'$ is obtained by adding the sub-pixel position $\hat{\overrightarrow{v}}_{s,sub}$ with the remaining discrete displacement $\hat{\overrightarrow{v_s}}$. The interpolation block size was chosen by analyzing the quality of the sub-pixelic result. The initial neighbourhood is a $3 \times 3$ block. If the sub position estimation is not in the interval $-0.33 < \hat{\overrightarrow{v}}'_{s,sub} < 0.33$, the interpolation is re-computed over a $5 \times 5$ block. Next, if the candidate is not in the interval $-0.5 < \hat{\overrightarrow{v}}'_{s,sub} < 0.5$, it is rejected.

## 4. EXPERIMENTS AND RESULTS

The two local estimators presented in section 2 have been applied on two SAR images of the lower part of the glacier of Argentière (French Alps) sensed by TerraSAR-X on September 29th, 2008 and October 10th, 2008 respectively. The two SAR images have been previously co-registered on static areas. They have a resolution cell of $1.36 \times 2.04$ meters in line of sigh (LOS) and azimuth directions respectively. Search windows of size $13 \times 13$ were used. This corresponds on a maximum displacement of about $56$ cm/day and on the size of interpolation window. Patches of size $101 \times 101$ (neighborhoods of $t$ and $s$) were chosen, i.e. about 228 m and 202 m in ground geometry. A binary mask was provided to localize the glacier surface. Figure 2 shows the estimated NCC and ML displacement field obtained from the two amplitude images of the glacier surface. At each position is represented the magnitude and the orientation angle of the local displacement. The displacement is well recovered by both methods in regions where there is texture information such as the areas with crevasses. The global direction follows the movement of the glacier with a maximum speed in the breaking slope of "Lognan serac falls".

Table 1 presents confidence and displacement measure statistics performed on this pair of SAR images. The $h_{peak}$ statistics are computed over the given binary mask. The NCC and ML displacement statistics are computed over a $100 \times 100$ block on a higher crevasses area (zone 1) and a lower crevasses area (zone 2). The $h_{peak}$ mean shows that the NCC approach provides a better confidence than the ML approach. However, the $h_{peak}$ standard deviation (std) is lower for the ML approach. The NCC and ML displacement means are relatively close but the ML estimate presents a smaller standard deviation. The ML displacement distribution is thus finer, and consequently the ML approach can be considered as more accurate than the NCC approach.

## 5. CONCLUSION

A new estimator for glacier monitoring is proposed. Displacement vectors are estimated based on the similarity between patches extracted from two SAR images co-registered on static areas and sensed at different times. Patch similarity is expressed as the likelihood that two patches have the same underlying reflectivity given the observed noisy amplitude patches. This similarity, proposed originally in [7], deals well with multiplicative speckle noise. These similarities are then used in the maximum likelihood estimator which is efficient in several situations. The comparison with classical correlation based tracking proves that the ML estimator is the most accurate approach. However, the experiment shows that the ML confidence is lower than the NCC approach.

## 6. REFERENCES


[1] T. Strozzi, A. Luckman, T. Murray, U. Wegmuller, and C.L. Werner, "Glacier motion estimation using SAR offset-tracking procedures," *IEEE Transactions on Geoscience and Remote Sensing*, vol. 40, no. 11, pp. 2384–2391, 2002.

[2] E. Erten, A. Reigber, O. Hellwich, and P. Prats, "Glacier Velocity Monitoring by Maximum Likelihood Texture Tracking," *IEEE Transactions on Geoscience and Remote Sensing*, vol. 47, no. 2, pp. 394–405, 2009.

[3] B. Zitová and J. Flusser, "Image registration methods: a survey," *Image and Vision Computing*, vol. 21, no. 11, pp. 977–1000, 2003.

[4] E. Berthier, H. Vadon, D. Baratoux, Y. Arnaud, C. Vincent, K.L. Feigl, F. Rémy, and B. Legrésy, "Mountain glaciers surface motion derived from satellite optical imagery," *Remote Sensing Environ.*, vol. 95, no. 1, pp. 14–28, 2005.

[5] D. Scherler, S. Leprince, and R. Manfred ans R. Strecker, "Glacier-surface velocities in alpine terrain from optical satellite imagery - Accuracy improvement and quality assessment," *Remote Sensing of Environment*, vol. 112, no. 10, pp. 3806–3819, 2008.

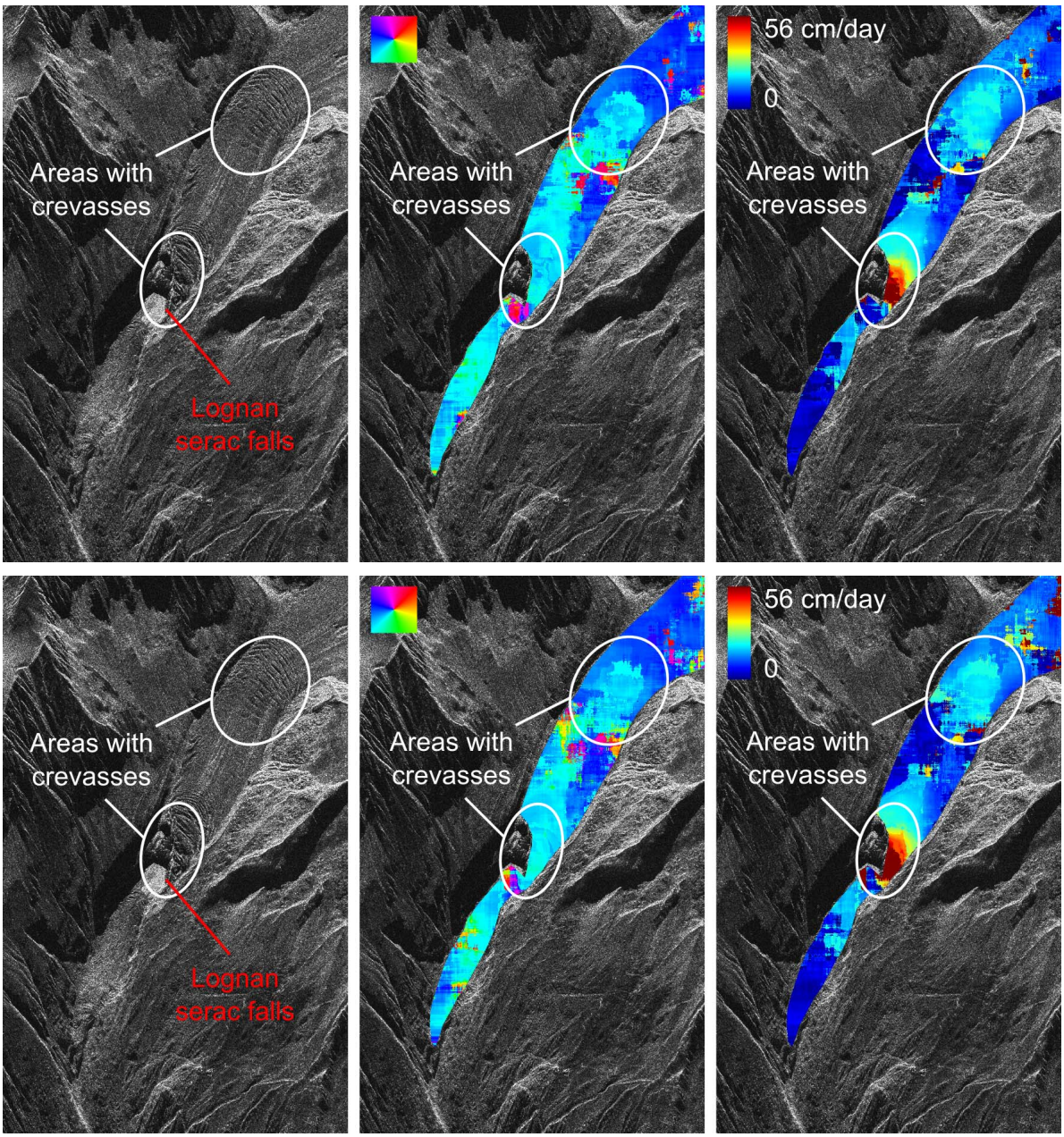


**Fig. 2**. (left) SAR image of the glacier of Argentière, (center) orientations and (right) speeds of the displacement given by the maximum likelihood estimator. (top) The NCC estimation and (bottom) the ML estimation. Both estimators provide likely result: the global direction follows the movement of the glacier with a maximum speed in the breaking slope of "Lognan serac falls".

[6] D.J. Quincey, L. Copland, C. Mayer, M. Bishop, A. Luckman, and M. Belò, "Ice velocity and climate variations for Baltoro glacier, Pakistan," *Journal of Glaciology*, vol. 55, no. 194, pp. 596–606, 2009.

[7] C.A. Deledalle, L. Denis, and F. Tupin, "Iterative Weighted Maximum Likelihood Denoising with Probabilistic Patch-Based Weights," *IEEE Transactions on Image Processing*, vol. 18, no. 12, pp. 2661–2672, 2009.

[8] K. Nakamura, K. Doi, and K. Shibuya, "Estimation of seasonal changes in the flow of Shirase glacier using JERS-1/SAR image correlation," *Polar Science*, vol. 1, no. 2-4, pp. 73–83, 2007.